Hindawi
Complexity
Volume 2018, Article ID 8797314, 12 pages
https://doi.org/10.1155/2018/8797314

Research Article

Dynamics Feature and Synchronization of a Robust Fractional-Order Chaotic System

Xuan-Bing Yang,[1,2] Yi-Gang He,[1] and Chun-Lai Li[2]

[1] *School of Electrical Engineering and Automation, Hefei University of Technology, Hefei 230009, China*
[2] *School of Information Science and Engineering, Hunan Institute of Science and Technology, Yueyang 414006, China*

Correspondence should be addressed to Yi-Gang He; 18655136887@163.com and Chun-Lai Li; hnistlichl@163.com

Received 20 September 2018; Accepted 6 November 2018; Published 2 December 2018

Guest Editor: Viet-Thanh Pham

Exploring the dynamics feature of robust chaotic system is an attractive yet recent topic of interest. In this paper, we introduce a three-dimensional fractional-order chaotic system. The important finding by analysis is that the position of signal x_3 descends at the speed of $1/c$ as the parameter b increases, and the signal amplitude of x_1, x_2 can be controlled by the parameter m in terms of the power function with the index $-1/2$. What is more, the dynamics remains constant with the variation of parameters b and m. Consequently, this system can provide rich encoding keys for chaotic communication. By considering the properties of amplitude and position modulation, the partial projective synchronization and partial phase synchronization are realized with linear control scheme. The distribution map of optimal synchronization region in the control-parameter space is charted by defining the power consumption of controller. Numerical simulations are executed to confirm the theoretical analysis.

1. Introduction

Over the past few decades, the dynamics and property of chaotic system have been extensively studied from different points of views as an active topic [1–4]. The investigation of chaos has benefited the exploration of the complex behavior, intrinsic nonlinear structure of natural system, and the construction of chaotic system, as well as practical applications such as secure communications and signal detection [5–9]. Robust chaotic system can usually provide signal-amplitude modulation by controlling one or some of the parameters in the dynamical equations yet keep the Lyapunov exponents and power spectral density invariable [10–14]. Therefore, it is a type of chaotic system with potential applications in synchronization, signal processing, image encryption, chaotic radar, and chaotic communication [10, 12]. However, according to what we know, there is little information and variety about such system reported in the present literatures.

Although fractional calculus has a history of more than 300 years, it was not really applied to physics, life sciences, and psychology until the last decade [15–18]. Fractional calculus can provide an excellent description of hereditary and memory properties in various materials and processes. The advantage of the fractional system is that it holds more degrees of freedom and that contains a "memory" in it. Therefore, it is of universal significance to study fractional dynamics and its applications [19–22]. Synchronization of integer-order chaotic system is investigated extensively and deeply, and many different types and methods have been presented since the landmark work by Pecora and Carroll [23–29]. However, due to the computational complexity of fractional systems, not all synchronization methods of the integer-order system are suitable for the fractional-order one [10]. In the existing synchronization types, projective synchronization can be interpreted as that the state trajectories of the drive and response systems synchronize to a constant proportion factor. This characteristic is usually used to extend binary digital communication to faster M-nary communication [30, 31]. Another synchronization type to be worth mentioning is phase synchronization, in which the controlled chaotic system adjusts the signal frequencies of dynamics to the rhythm of another chaotic system while the amplitudes go on varying in an irregular and uncorrelated fashion [32]. Phase synchronization has been observed in electrochemical oscillators [33], plasma discharge tubes [34], coupled HR neurons [35], fractional differential chaotic systems [36], etc.

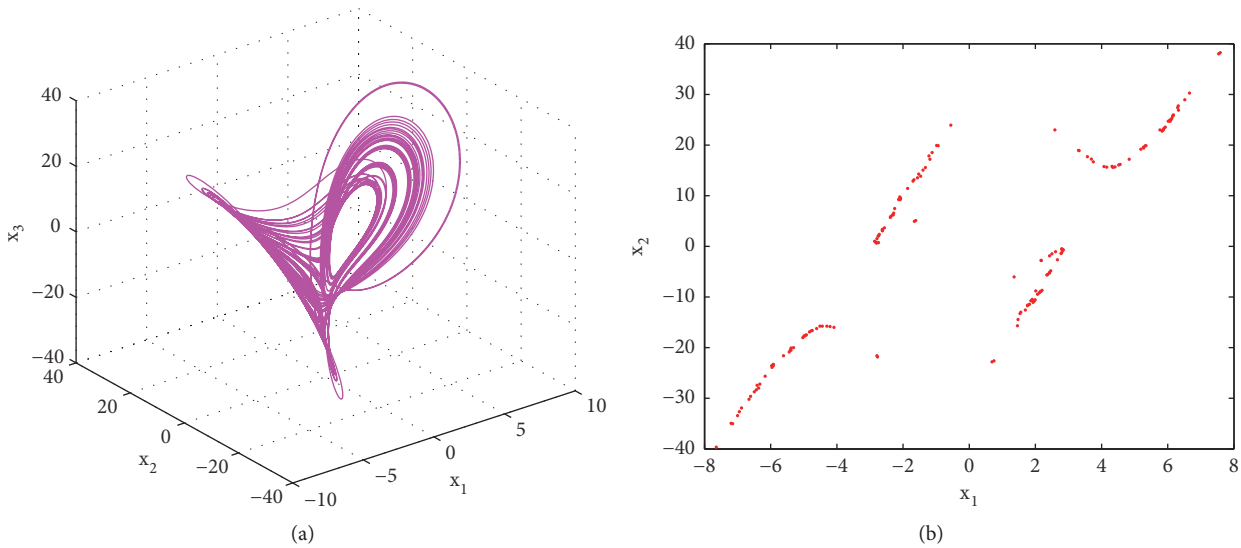

Figure 1: (a) 3D phase portrait; (b) Poincaré map with x_3=0.6.

In this paper, we attempt to explore some new dynamics properties of robust chaotic system by constructing a three-dimensional fractional chaotic system and to further consider the synchronization problem. Analysis of the derived system shows that the parameter m can control the signal amplitude of x_1, x_2 by the power function with the index $-1/2$ and that the parameter b can control the position of signal x_3 at the descent velocity of $1/c$. Then, by considering the vital property of amplitude and position modulation, a linear coupling scheme is designed to realize the partial projective synchronization and partial phase synchronization, respectively. Thus, the proportional factors in projective synchronization and the phase feature in phase synchronization are only determined by system parameters, which will improve the security of synchronous communication. The coupling-parameter range for synchronization is derived analytically and can be effectively narrowed down by appropriately selecting the auxiliary parameters. The distribution map of optimal synchronization region in the coupling-parameter space is further evaluated by defining the power consumption of controller. Numerical simulations are shown to further confirm the theoretical analysis.

2. Model of Fractional-Order Chaotic System

2.1. Model Description. The introduced fractional system is written in the form

$$\begin{aligned} D^q x_1 &= x_2 - a x_1 \\ D^q x_2 &= -b x_1 - c x_1 x_3 \\ D^q x_3 &= -n + m x_1 x_2 \end{aligned} \tag{1}$$

In system (1), $D^q x = d^q x/dt^q$ denotes the Caputo fractional derivative with the initial time $t = 0$ [37]. With the positive parameters a, b, c, n, and m, two equilibrium points of system (1) are obtained as

$$\begin{aligned} &E_+\left(\sqrt{\frac{n}{am}}, \sqrt{\frac{an}{m}}, -\frac{b}{c}\right), \\ &E_-\left(-\sqrt{\frac{n}{am}}, -\sqrt{\frac{an}{m}}, -\frac{b}{c}\right). \end{aligned} \tag{2}$$

The corresponding characteristic equation for any equilibrium point (x_{E1}, x_{E2}, x_{E3}) can be deduced as

$$\begin{aligned} \varphi(\lambda) = &-\lambda^3 - a\lambda^2 - \left(b + c x_{E3} + c m {x_{E1}}^2\right)\lambda \\ &- a c m {x_{E1}}^2 - c m x_{E1} x_{E2} \end{aligned} \tag{3}$$

Specially, when selecting the parameter set $P = \{a = 2, b = 1, c = 1, n = 30, m = 1\}$, the corresponding equilibrium points and characteristic roots are

$$\begin{aligned} &E_+(3.873, 7.746, -1): \\ &\lambda_1 = -3.1912, \\ &\lambda_2 = 0.5956 + 4.2950i, \\ &\lambda_3 = 0.5956 - 4.2950i \\ &E_-(-3.873, -7.746, -1): \\ &\lambda_1 = -3.1912, \\ &\lambda_2 = 0.5956 + 4.2950i, \\ &\lambda_3 = 0.5956 - 4.2950i \end{aligned} \tag{4}$$

With the aid of stability theory of commensurate fractional system [38], the necessary condition for the chaos emergence is $q > (2/\pi)\mathrm{atan}(|\mathrm{Im}(\lambda*)|/\mathrm{Re}(\lambda*)) = (2/\pi)\mathrm{atan}(4.295/0.5956) = 0.9123$. For the parameter set P and the fractional order q=0.96, the 3D phase diagram and Poincaré map with dense dots are shown in Figure 1, revealing that system (1) is indeed chaotic.

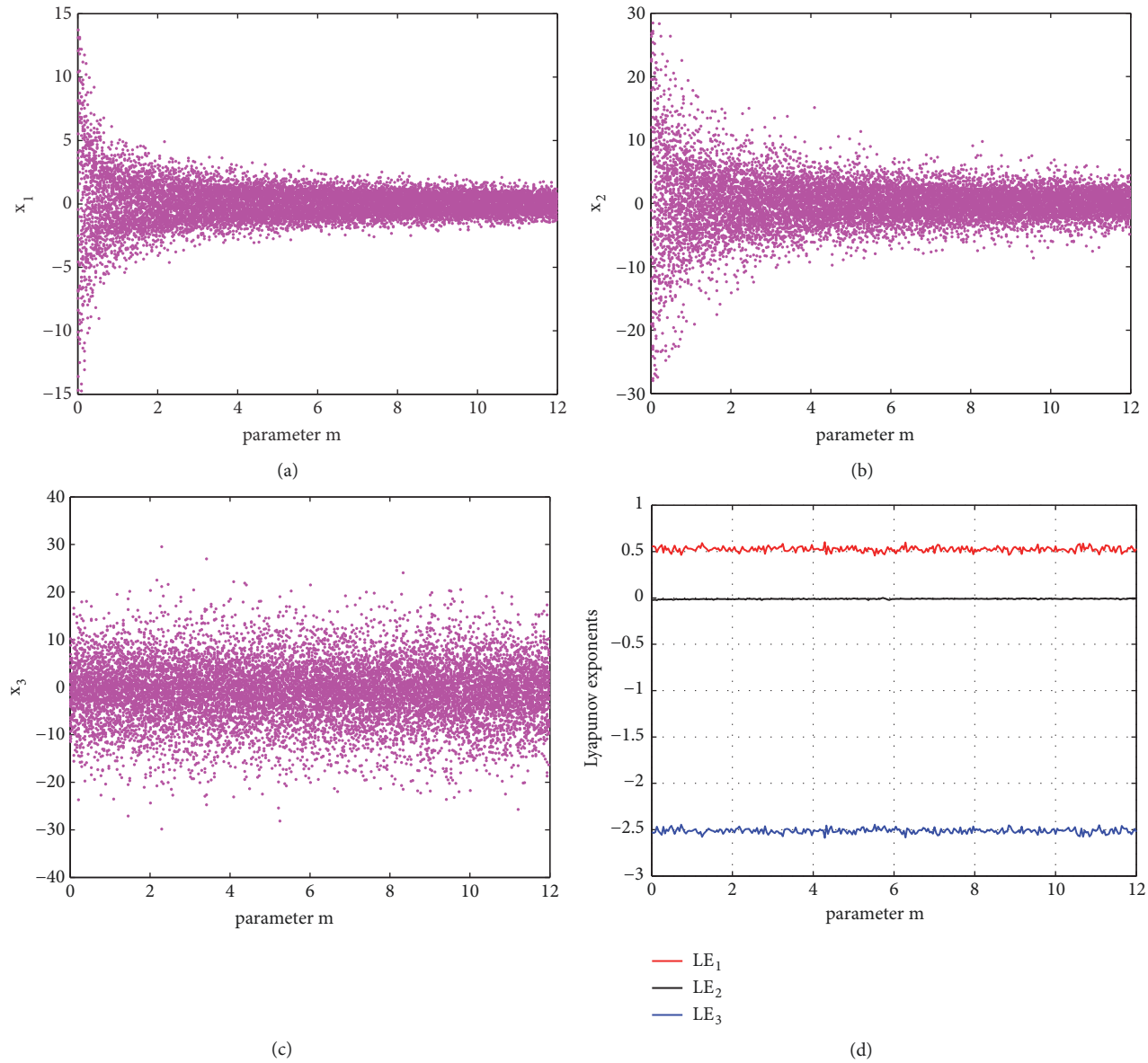

Figure 2: (a), (b), and (c) Bifurcation diagram and (d) Lyapunov exponent spectrum versus parameter m.

2.2. Dynamics Feature of Amplitude and Position Modulation. Our analysis found that the introduced system has the robust chaos of constant Lyapunov exponents with the variation of parameters m and b. More specifically, the parameter m can control some of the signal amplitude of state variables, and the parameter b can control the position of one of the variables with a certain speed. The revealed feature is rare in the current literature and we believe it will stimulate an exploration boom.

The linear transformation of $x_1 \longrightarrow x_1/\sqrt{m}$, $x_2 \longrightarrow x_2/\sqrt{m}$, and $x_3 \longrightarrow x_3$ is first considered to deduce system (1) to the normalized form about parameter m [12], as follows:

$$\begin{aligned} D^q x_1 &= x_2 - a x_1 \\ D^q x_2 &= -b x_1 - c x_1 x_3 \\ D^q x_3 &= -n + x_1 x_2 \end{aligned} \tag{5}$$

Therefore, the control parameter m can modulate the signal amplitude of variables x_1, x_2 according to $1/\sqrt{m}$, but the signal x_3 keeps its amplitude constant.

We substitute the nonzero equilibrium point E_+ or E_- into characteristic equation (3) to obtain

$$\varphi(\lambda) = -\lambda^3 - a\lambda^2 - \frac{cn}{a}\lambda - 2cn \tag{6}$$

Since (6) is irrespective to parameter m, the Lyapunov exponent spectrum remains invariable when m increases. The dynamics feature of amplitude modulation for system (1) is illustrated by bifurcation diagram and Lyapunov exponent spectrum, as shown in Figure 2. In the figure, the bifurcation diagrams are plotted with the local maxima of variables versus control parameter, and the spectrum of Lyapunov exponents is calculated by the wolf method.

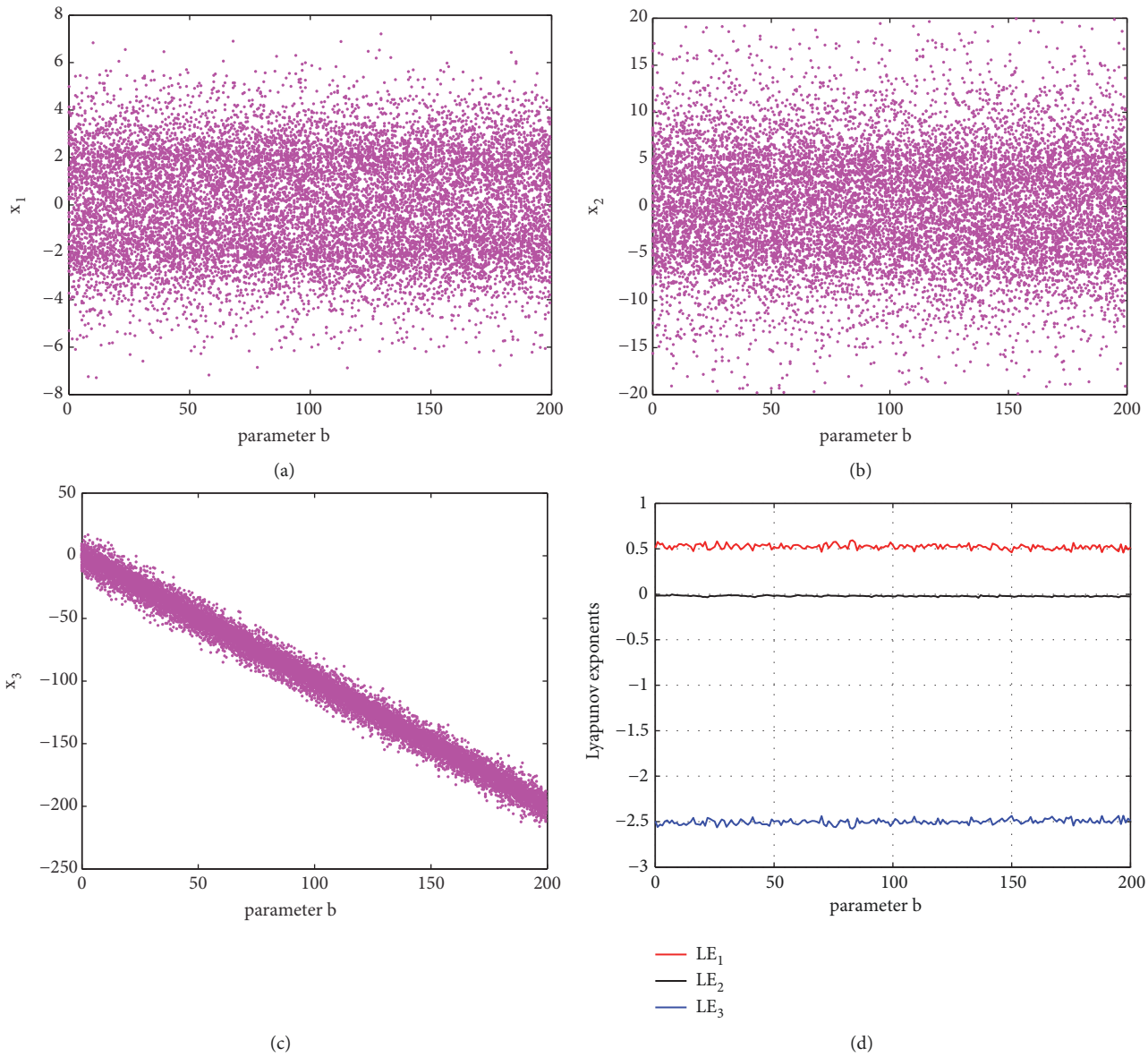

Figure 3: (a), (b), and (c) Bifurcation diagram and (d) Lyapunov exponent spectrum versus parameter b with the parameter set P except for b.

When introducing the linear transformation of $x_1 \longrightarrow x_1$, $x_2 \longrightarrow x_2$, and $x_3 \longrightarrow x_3 + k_p/c$, we then deduce system (1) to

$$\begin{aligned} D^q x_1 &= x_2 - a x_1 \\ D^q x_2 &= -\left(b + k_p\right) x_1 - c x_1 x_3 \\ D^q x_3 &= -n + m x_1 x_2 \end{aligned} \tag{7}$$

Therefore, the position of signal x_3 descends at the speed of $1/c$ as the parameter b increases, while the signals x_1, x_2 keep their amplitude invariable. Similarly, it is known that (6) is also irrespective to parameter b. Thus, the spectrum of Lyapunov exponent remains constant when b varies in field of real number. The phenomenon of position modulation for system (1) is described by bifurcation diagram and Lyapunov exponent spectrum, as shown in Figure 3. And the speed of position modulation influenced by parameter c is interpreted in Figure 4 by the bifurcation diagram and the maximal Lyapunov exponent spectrum, which signifies that a smaller c will give rise to a larger descent velocity.

3. Preliminaries for Synchronization of Fractional Chaotic System

In this section, some concepts and techniques are recalled for the stability analysis of fractional system.

Definition 1 (see [39]). When function $\alpha : R^+ \longrightarrow R^+$ is continuous, strictly increasing, and $\alpha(0) = 0$, it is said to be

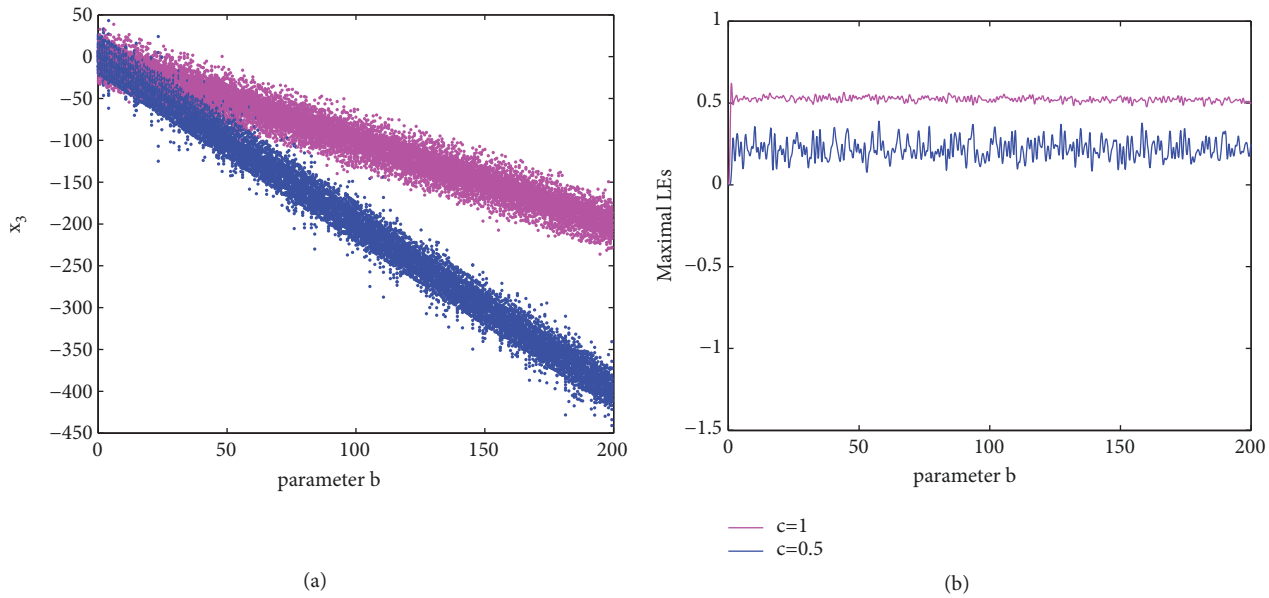

FIGURE 4: Influence of c on position modulation interpreted by (a) Bifurcation diagram and (b) Lyapunov exponent spectrum versus b with c=1 in magenta and c=0.5 in blue.

of class κ. If $\alpha \in \kappa$ and satisfies $\alpha(t) \longrightarrow \infty$ with $t \longrightarrow \infty$, it is said that α is of class κ_∞.

Lemma 2 (see [40, 41]). *Let $z(t) \in R$ be a continuous and derivable function. Then, for any time instant $t \geq 0$, it is held:*

$$0.5D^q z^2(t) \leq z(t) D^q z(t), \quad \forall q \in (0,1) \tag{8}$$

Lemma 3 (see [42, 43]). *Let $z(t) \in R^n$ be a real-valued continuous and derivable vector function. Then, for any time instant $t \geq 0$, one will always hold the following inequality:*

$$\begin{gathered} 0.5D^q z^T(t) Pz(t) \leq z^T(t) PD^q z(t), \\ \forall q \in (0,1), \ P = \operatorname{diag}(p_1, p_2, \cdots, p_n) > 0 \end{gathered} \tag{9}$$

Theorem 4 (Lyapunov stability and uniform stability of fractional system [42]). *Considering the following fractional-order system with the Caputo definition*

$$D^q z(t) = f(z,t), \quad q \in (0,1) \tag{10}$$

Let z=0 be an equilibrium point of system (10). If there exists a continuous Lyapunov function $V(z,t)$ and a scalar class-K function α_1 satisfying

$$V(z,t) \geq \alpha_1(\|z(t)\|) \tag{11}$$

and

$$D^q V(z,t) \leq 0, \quad q \in (0,1) \tag{12}$$

for any $z \neq 0$, then system (10) is Lyapunov stable at $z = 0$.

Furthermore, if there exists another scalar class-K function α_2 such that

$$V(z,t) \leq \alpha_2(\|z(t)\|) \tag{13}$$

then the origin of system (10) is said to be Lyapunov uniformly stable.

4. Partial Projective Synchronization of Fractional Chaotic System

4.1. Synchronization Scheme. The partial projective synchronization of the proposed system is studied here by taking the advantage of the property of amplitude modulation.

Let system (1) be as the drive system, and the response system is expressed as

$$\begin{aligned} D^q y_1 &= y_2 - ay_1 \\ D^q y_2 &= -by_1 - cy_1 y_3 + u_2 \\ D^q y_3 &= -n + m_1 y_1 y_2 + u_3 \end{aligned} \tag{14}$$

where u_2 and u_3 are the controllers to be determined.

Assumption 5. The state variables of systems (1) and (14) are all bounded, and there exist three positive constants σ_1, σ_2, and σ_3, such that $|x_1|, |y_1| \leq \sigma_1$, $|x_2|, |y_2| \leq \sigma_2$, and $|x_3|, |y_3| \leq \sigma_3$.

The synchronization errors are set as $e_1 = y_1 - \sqrt{m/m_1}x_1$, $e_2 = y_2 - \sqrt{m/m_1}x_2$, and $e_3 = y_3 - x_3$, by taking the property of amplitude modulation considered. Then we obtain the error dynamical system

$$\begin{aligned} D^q e_1 &= e_2 - ae_1 \\ D^q e_2 &= -be_1 - cy_1 e_3 - ce_1 x_3 + u_2 \\ D^q e_3 &= m_1 y_2 e_1 + m_1 \sqrt{\frac{m}{m_1}} x_1 e_2 + u_3 \end{aligned} \tag{15}$$

Theorem 6. *For the drive system (1) and response system (14), the controllers are designed as $u_2 = -k_2 e_2$ and $u_3 = -k_3 e_3$. If the coupling parameters k_2 and k_3 satisfy*

$$k_2 > \frac{(p_1 - bp_2 + cp_2\sigma_3)^2}{4ap_1p_2} \tag{16}$$

$$k_3 > \frac{m_1p_3\sigma_2(p_1 - bp_2 + cp_2\sigma_3)\left(m_1p_3\sqrt{m/m_1}\sigma_1 + cp_2\sigma_1\right) + k_2p_2(m_1p_3\sigma_2)^2 + ap_1\left(m_1p_3\sqrt{m/m_1}\sigma_1 + cp_2\sigma_1\right)^2}{p_3\left(4ap_1p_2k_2 - (p_1 - bp_2 + cp_2\sigma_3)^2\right)} \tag{17}$$

where p_1, p_2, and p_3 are positive auxiliary parameters to narrow down the values range of the coupling parameters, then the partial projective synchronization is realized with Lyapunov uniformly stability.

Proof. Let us propose the Lyapunov function $V(t) = 0.5(p_1{e_1}^2 + p_2{e_2}^2 + p_3{e_3}^2)$, which satisfies $\alpha_1(\|e\|) \le V(t) \le \alpha_2(\|e\|)$ for $\alpha_1(\|e\|) = \lambda_{\min}(P)\|e\|^2$, $\alpha_2(\|e\|) = \lambda_{\max}(P)\|e\|^2$, and $P = \mathrm{diag}(p_1, p_2, p_3)$. Taking q-order fractional derivative with respect to time t along the trajectories of (15), it yields

$$\begin{aligned} D^qV(t) &= 0.5D^qp_1{e_1}^2 + 0.5D^qp_2{e_2}^2 + 0.5D^qp_3{e_3}^2 \\ &\le p_1e_1D^qe_1 + p_2e_2D^qe_2 + p_3e_3D^qe_3 \\ &= -ap_1{e_1}^2 - k_2p_2{e_2}^2 - k_3p_3{e_3}^2 \\ &\quad + (p_1 - bp_2 - cp_2x_3)e_1e_2 \\ &\quad + \left(m_1p_3\sqrt{\frac{m}{m_1}}x_1 - cp_2y_1\right)e_2e_3 \\ &\quad + m_1p_3y_2e_1e_3 \\ &\le -ap_1{e_1}^2 - k_2p_2{e_2}^2 - k_3p_3{e_3}^2 \\ &\quad + (p_1 - bp_2 + cp_2\sigma_3)|e_1||e_2| \\ &\quad + \left(m_1p_3\sqrt{\frac{m}{m_1}}\sigma_1 + cp_2\sigma_1\right)|e_2||e_3| \\ &\quad + m_1p_3\sigma_2|e_1||e_3| = |e|^T\Pi|e| \end{aligned} \tag{18}$$

with

$$|e| = (|e_1|, |e_2|, |e_3|)^T,$$
$$\Pi = \begin{pmatrix} -ap_1 & \frac{p_1 - bp_2 + cp_2\sigma_3}{2} & \frac{m_1p_3\sigma_2}{2} \\ \frac{p_1 - bp_2 + cp_2\sigma_3}{2} & -p_2k_2 & \frac{m_1p_3\sqrt{m/m_1}\sigma_1 + cp_2\sigma_1}{2} \\ \frac{m_1p_3\sigma_2}{2} & \frac{m_1p_3\sqrt{m/m_1}\sigma_1 + cp_2\sigma_1}{2} & -p_3k_3 \end{pmatrix}. \tag{19}$$

It requires $\Pi \le 0$ for catering to $D^qV(t) \le 0$. Thus we have

$$\begin{aligned} \Delta_1 &= -ap_1 \le 0 \\ \Delta_2 &= \det\begin{pmatrix} -ap_1 & \frac{p_1 - bp_2 + cp_2\sigma_3}{2} \\ \frac{p_1 - bp_2 + cp_2\sigma_3}{2} & -p_2k_2 \end{pmatrix} \ge 0 \\ \Delta_3 &= \det\begin{pmatrix} -ap_1 & \frac{p_1 - bp_2 + cp_2\sigma_3}{2} & \frac{m_1p_3\sigma_2}{2} \\ \frac{p_1 - bp_2 + cp_2\sigma_3}{2} & -p_2k_2 & \frac{m_1p_3\sqrt{m/m_1}\sigma_1 + cp_2\sigma_1}{2} \\ \frac{m_1p_3\sigma_2}{2} & \frac{m_1p_3\sqrt{m/m_1}\sigma_1 + cp_2\sigma_1}{2} & -p_3k_3 \end{pmatrix} \le 0 \end{aligned} \tag{20}$$

Therefore, we finally obtain inequalities (16) and (17). This completes the proof. □

4.2. Simulation Analysis. The appropriate selection of parameters p_1, p_2, and p_3 can effectively narrow down the values

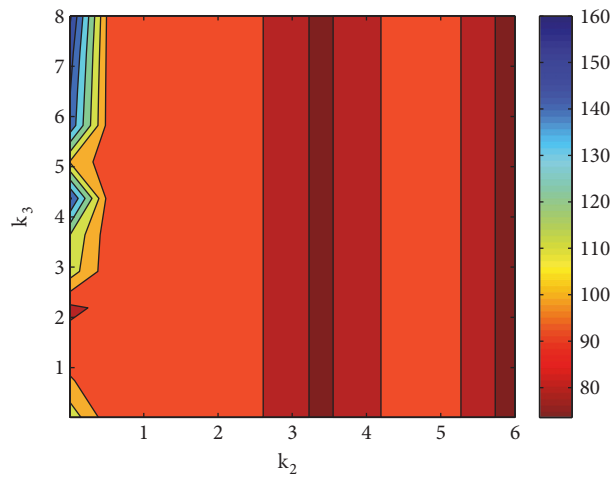

Figure 5: The distribution of the maximal power consumption of synchronous controller.

range of the coupling parameters, which is useful in actual synchronization process. However, it is a complicated relation between the coupling strengths (k_2, k_3) and (p_1, p_2, p_3). To optimize the synchronization scheme, we will evaluate the distribution map of optimal synchronization region in the coupling-parameter space, by coopting the idea introduced by Ma [44]. We first define the power consumption of the synchronous systems as $p_d = |x_1x_3|$ and $p_r = |y_1y_3|$, respectively. Thus, the power consumption for evaluating the synchronous controller can be defined as

$$p_{syn} = \left| |y_1y_3| - \sqrt{\frac{m}{m_1}}\,|x_1x_3| \right| \tag{21}$$

And for the sake of simplicity, we only consider the maximal power consumption of synchronous controller, as below

$$p_{msyn} = \max\left(p_{syn}\right) \tag{22}$$

Therefore, the optimal synchronization region will be the coupling-parameter region (k_2, k_3) with the minimum p_{msyn}.

In the numerical analysis, we choose the parameter values as a=2, b=1, c=1, n=30, m=1, m_1=16, and q=0.96 and set the initial values of drive system and the response system as $x(0)$=(-0.2, 0.1, 0.5), $y(0)$=(0.6, -0.5, -0.2). The distribution about the maximal power consumption of synchronous controller in the coupling-parameter space (k_2, k_3) is illustrated in Figure 5. It is known that the power consumption p_{msyn} is mainly determined by the coupling parameter k_2, and the optimal synchronization region appears alternately as k_2 increases. But to get shorter synchronous transition time, larger values of k_2 and k_3 are more appropriate.

The synchronization result with k_2=3.3, k_3=0.6 is depicted in Figure 6, which provides the proportional factors $\alpha_1 = \sqrt{m/m_1} = 0.25$, $\alpha_2 = \sqrt{m/m_1} = 0.25$, and $\alpha_3 = 1$. Figure 7 shows the synchronization result with the same proportional factors, when k_2=6, k_3=8. The comparative analysis shows that larger parameters k_2 and k_3 will lead to shorter synchronous transition time.

5. Partial Phase Synchronization of Fractional Chaotic System

5.1. Synchronization Scheme. Select the drive system (1) and the following response system:

$$\begin{aligned} D^q y_1 &= y_2 - ay_1 \\ D^q y_2 &= -b_1 y_1 - cy_1 y_3 + u_2 \\ D^q y_3 &= -n + my_1 y_2 + u_3 \end{aligned} \tag{23}$$

And when considering the property of position modulation, the errors of partial phase synchronization are expressed as $e_1 = y_1 - x_1$, $e_2 = y_2 - x_2$, and $e_3 = y_3 - x_3 + (b_1 - b)/c$, then the error dynamical system is obtained as

$$\begin{aligned} D^q e_1 &= e_2 - ae_1 \\ D^q e_2 &= -be_1 - cy_1 e_3 - ce_1 x_3 + u_2 \\ D^q e_3 &= me_1 y_2 + mx_1 e_2 + u_3 \end{aligned} \tag{24}$$

Theorem 7. *For the drive system (1) and response system (23), the controllers are designed as $u_2 = -k_2e_2$, $u_3 = -k_3e_3$. If the coupling parameters k_2 and k_3 satisfy the condition*

$$k_2 > \frac{(p_1 - bp_2 + cp_2\sigma_3)^2}{4ap_1p_2} \tag{25}$$

$$k_3 \geq \frac{mp_3\sigma_2(mp_3\sigma_1 + cp_2\sigma_1)(p_1 - bp_2 + cp_2\sigma_3) + k_2p_2(mp_3\sigma_2)^2 + ap_1(mp_3\sigma_1 + cp_2\sigma_1)^2}{4ap_1p_2p_3k_2 - p_3(p_1 - bp_2 + cp_2\sigma_3)^2} \tag{26}$$

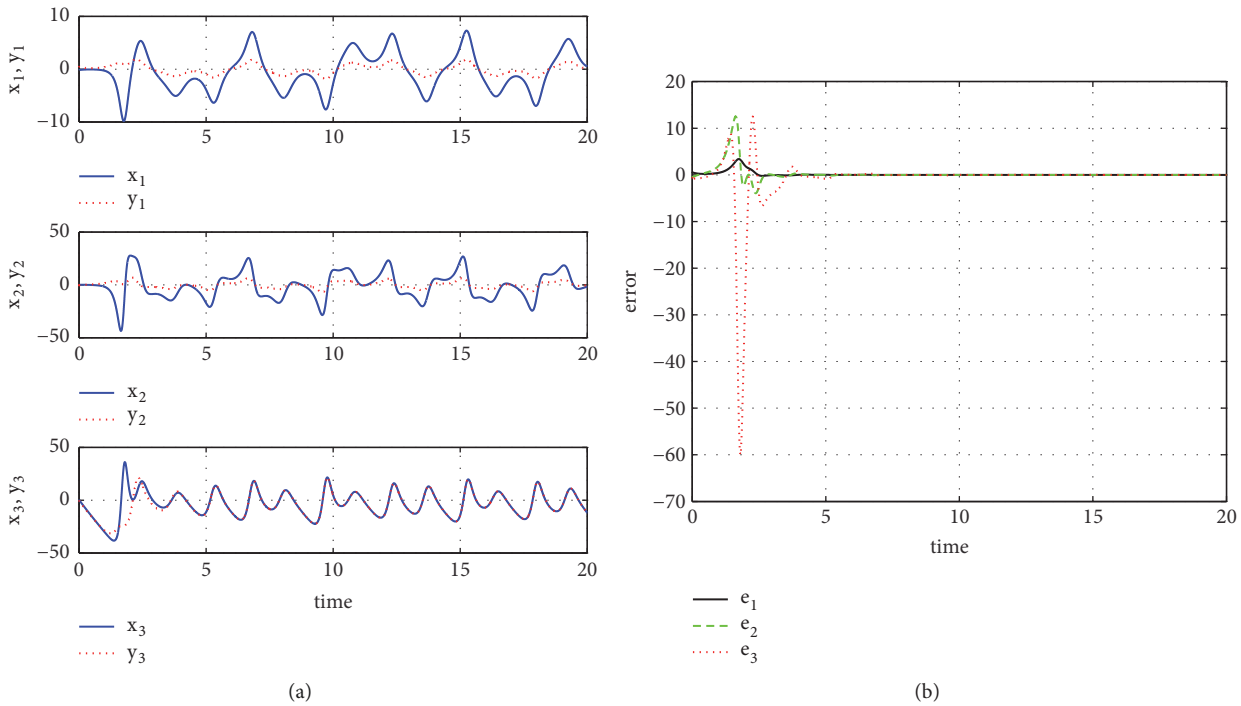

FIGURE 6: Partial projective synchronization with k_2=3.3; k_3=0.6: (a) time response; (b) synchronization error.

where p_1, p_2, and $p_3$are positive constants, then the partial phase synchronization is realized with Lyapunov uniformly stability.

Here we skip the proof process for brevity since it resembles the one of Theorem 6.

5.2. Simulation Analysis. Likewise, to effectively evaluate the optimal synchronization region, we consider the distribution of coupling parameters by defining the maximal power consumption of synchronous controller, as follows:

$$p_{msyn} = \max\left(\left|\left|y_1 y_3\right| - \left|x_1\left(x_3 - \frac{(b_1 - b)}{c}\right)\right|\right|\right) \quad (27)$$

In the numerical analysis, we choose the parameter values as a=2, b=1, c=1, n=30, m=1, b_1=12, and q=0.96 and set the initial values of drive system and the response system as $x(0)$=(-0.2, 0.1, 0.5), $y(0)$=(0.6, -0.5, -0.2). The distribution map about the maximal power consumption of synchronous controller in the coupling-parameter space (k_2, k_3) is illustrated in Figure 8. It is found that the distribution of p_{msyn} is complicated when k_2 is less than 4, and there exists an optimized coupling-parameter region near k_2=1. When k_2 continues to increase with the condition of $k_3 > 1$, the value of p_{msyn} gradually decreases, and finally it keeps in the optimal synchronization region with $k_2 > 9$.

As the examples to explain our analysis, we select two sets of coupling parameters (k_2=1, k_3=4) and (k_2=10, k_3=4) to realize the optimal synchronization. It can be found that we can realize the partial phase synchronization of fractional chaotic system with the selected coupling parameters, but larger parameters k_2 and k_3 will lead to shorter synchronous transition time, as illustrated in Figures 9 and 10. Further, to analyze the influence of c on the difference between various states of synchronized systems, the representative process of phase synchronization when k_2=10, k_3=4, and c=0.5 is considered, as shown in Figure 11. The graphs in Figures 10 and 11 signify that a smaller c will lead to a larger difference between the system variables of the phase synchronization.

6. Conclusion

Robust chaotic system is a recent research interest yet a promising candidate for signal processing, image encryption, chaotic radar, and chaotic communication. Therefore, it is worthwhile to explore the dynamics feature of robust chaotic system. In this paper, we introduced a robust fractional-order chaotic system and revealed the significant dynamics of position modulation and amplitude modulation.

The linear control scheme is designed to realize the partial projective synchronization and partial phase synchronization, by considering the property of amplitude and position modulation. The distribution of optimal synchronization region in the control-parameter space is evaluated by searching the minimum power consumption of the linear controller. Numerical experiments are executed to confirm the theoretical analysis. Since the relation of synchronization

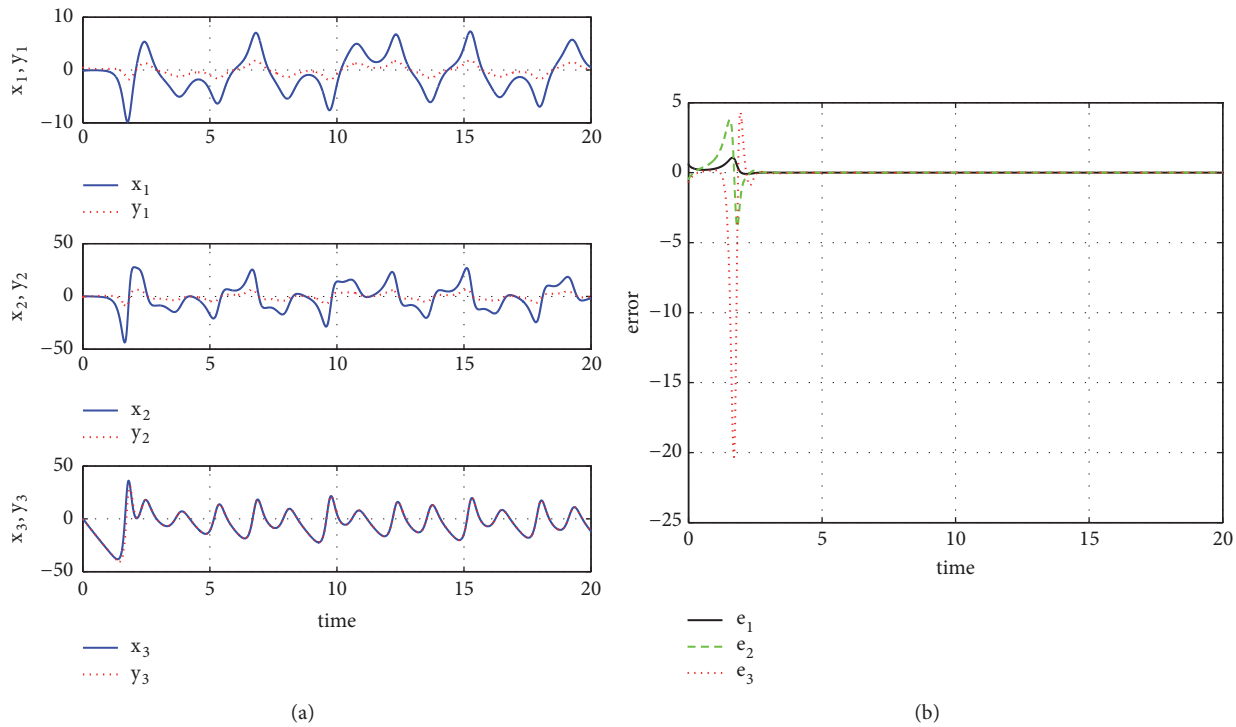

Figure 7: Partial projective synchronization with k_2=6; k_3=8: (a) time response; (b) synchronization error.

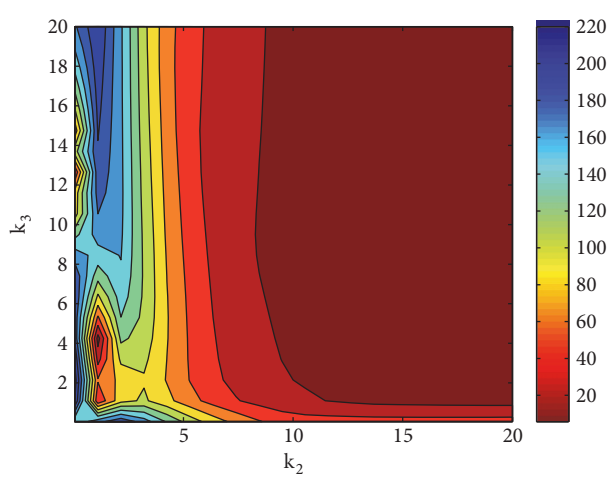

Figure 8: The distribution of the maximal power consumption of synchronous controller.

variables only depends on the system parameters, it is not easy to attack and accurately reconstruct the drive system. Therefore, it could be significant in secure communication for masking signals.

Data Availability

The data used to support the findings of this study are included within the article.

Conflicts of Interest

The authors declare that there are no conflicts of interest regarding the publication of this paper.

Acknowledgments

This work was supported by the National Natural Science Foundation of China under Grant no. 51577046, the

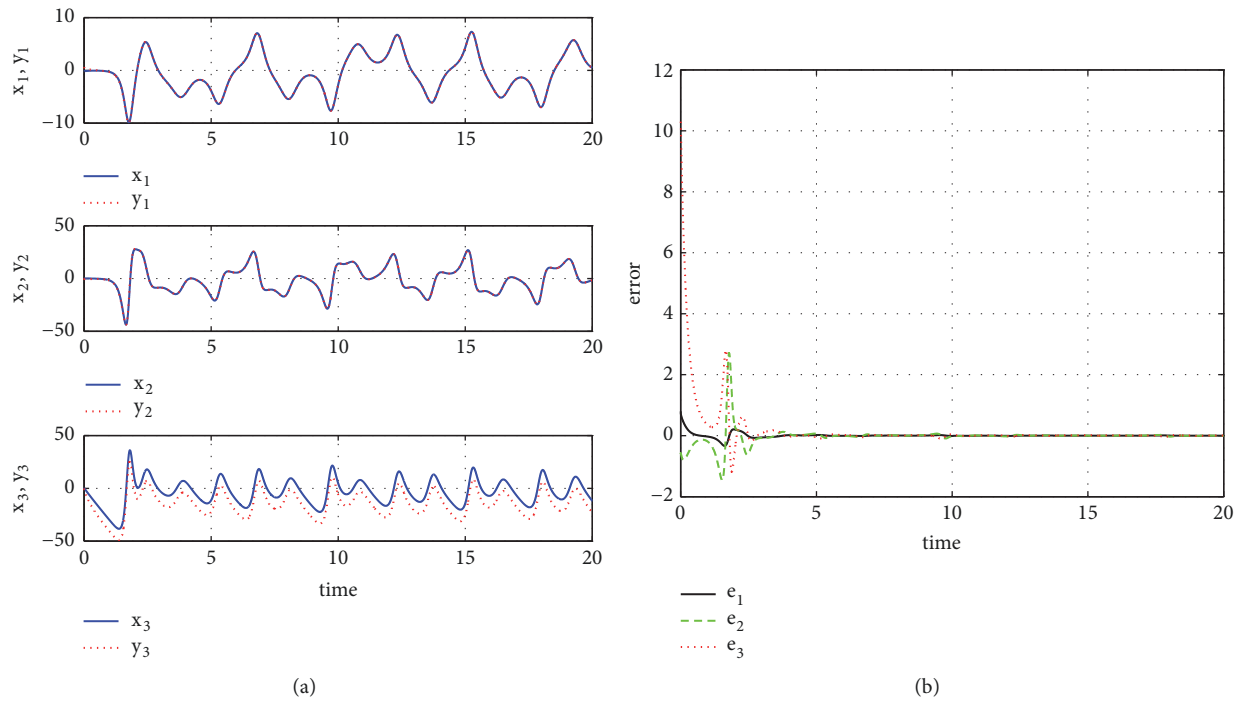

FIGURE 9: Partial phase synchronization with k_2=1; k_3=4: (a) time response; (b) synchronization error.

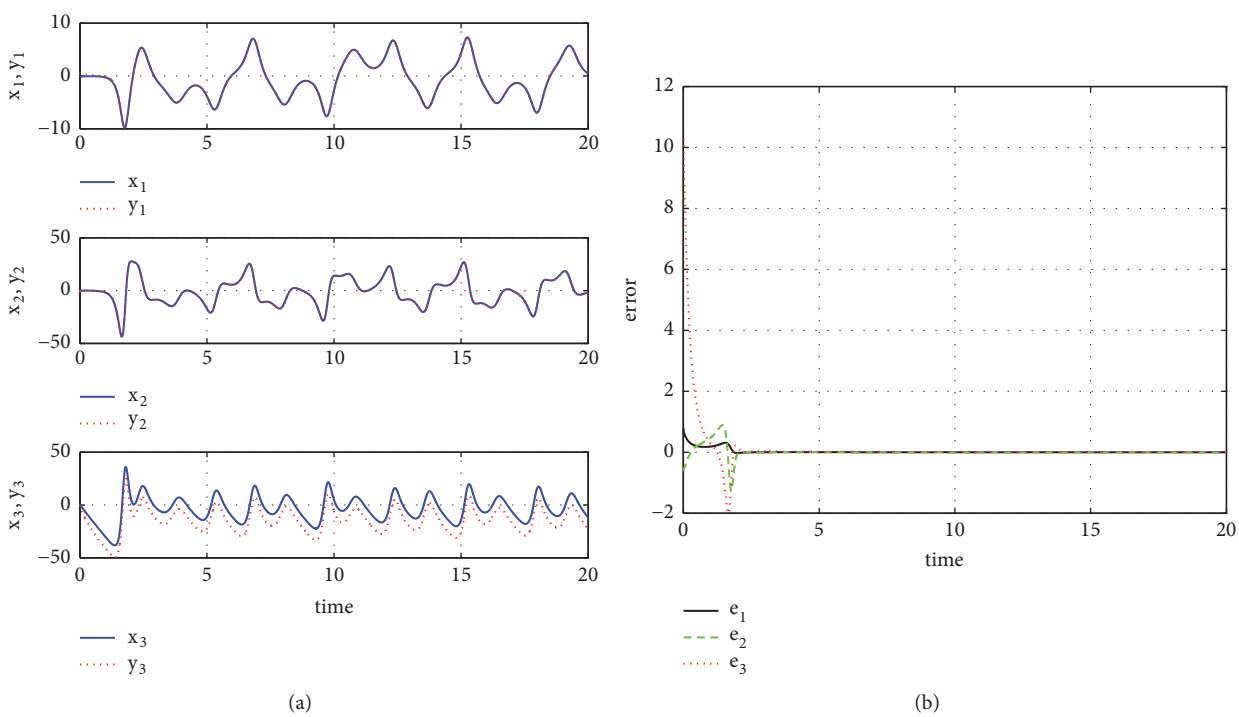

FIGURE 10: Partial phase synchronization with k_2=10, k_3=4, and c=1: (a) time response; (b) synchronization error.

State Key Program of National Natural Science Foundation of China under Grant no. 51637004, the National Key Research and Development Plan "Important Scientific Instruments and Equipment Development" under Grant no. 2016YFF0102200, Equipment Research Project in Advance under Grant no. 41402040301, the Research Foundation of Education Bureau of Hunan Province of China under Grant no. 16B113, and Hunan Provincial Natural Science Foundation of China under Grant no. 2016JJ4036.

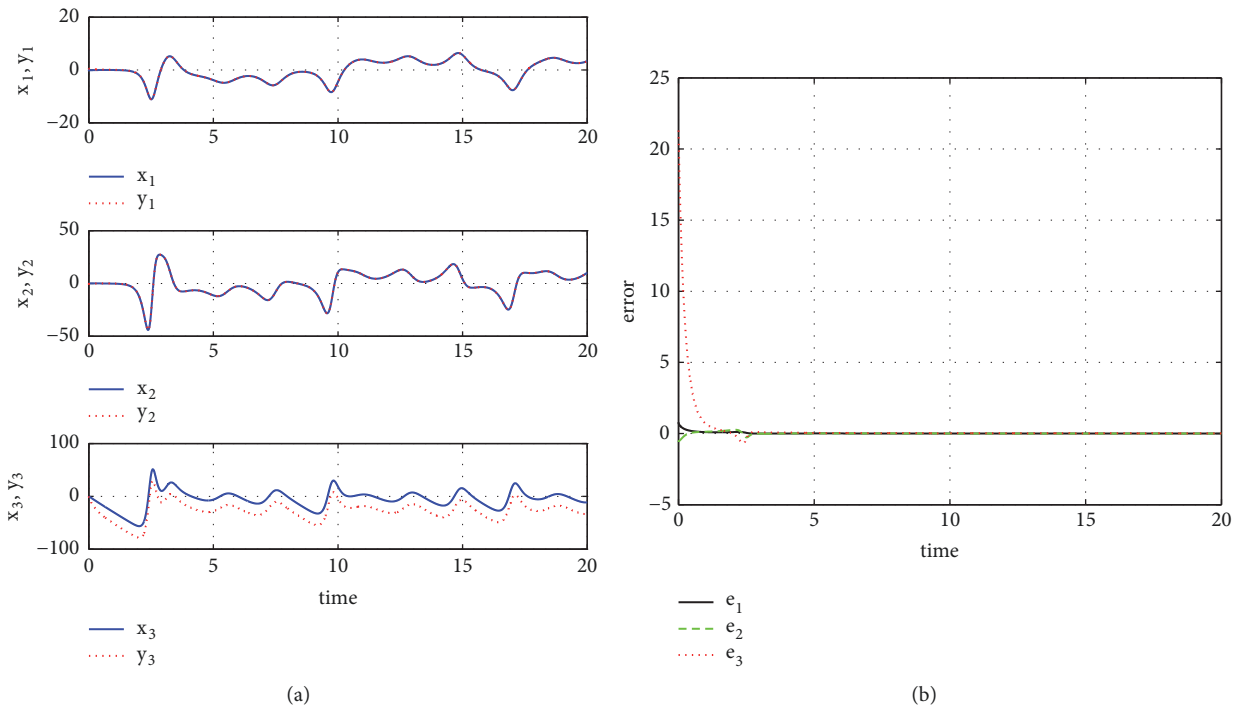

Figure 11: Partial phase synchronization with k_2=10, k_3=4, and c=0.5: (a) time response; (b) synchronization error.

References

[1] D. Kim, R. B. Gillespie, and P. H. Chang, "Simple, robust control and synchronization of the Lorenz system," *Nonlinear Dynamics*, vol. 73, no. 1-2, pp. 971–980, 2013.

[2] F. Peng, D.-L. Zhou, M. Long, and X.-M. Sun, "Discrimination of natural images and computer generated graphics based on multi-fractal and regression analysis," *AEUE - International Journal of Electronics and Communications*, vol. 71, pp. 72–81, 2017.

[3] Y. Li, D. Xu, Y. Fu, and J. Zhang, "Dynamic effects of delayed feedback control on nonlinear vibration isolation floating raft systems," *Journal of Sound and Vibration*, no. 13, pp. 2665–2676, 2014.

[4] L. Zhang, G. Cai, and X. Fang, "Stability for a novel time-delay financial hyperchaotic system by adaptive periodically intermittent linear control," *Journal of Information and Computing Science*, vol. 10, no. 3, pp. 189–198, 2015.

[5] Y. Zhao, X. Zhang, J. Xu, and Y. Guo, "Identification of chaotic memristor systems based on piecewise adaptive Legendre filters," *Chaos, Solitons & Fractals*, vol. 81, no. part A, pp. 315–319, 2015.

[6] H. Saberi Nik, S. Effati, and M. Shirazian, "An approximate-analytical solution for the Hamilton-Jacobi-Bellman equation via homotopy perturbation method," *Applied Mathematical Modelling*, vol. 36, no. 11, pp. 5614–5623, 2012.

[7] Y. Ji, X. Liu, and F. Ding, "New criteria for the robust impulsive synchronization of uncertain chaotic delayed nonlinear systems," *Nonlinear Dynamics*, vol. 79, no. 1, pp. 1–9, 2015.

[8] Y. Luo, M. Du, and J. Liu, "A symmetrical image encryption scheme in wavelet and time domain," *Communications in Nonlinear Science and Numerical Simulation*, vol. 20, no. 2, pp. 447–460, 2015.

[9] X. Xiang and B. Shi, "Weak signal detection based on the information fusion and chaotic oscillator," *Chaos: An Interdisciplinary Journal of Nonlinear Science*, vol. 20, no. 1, pp. 135–138, 2010.

[10] C. Li and J. Zhang, "Synchronisation of a fractional-order chaotic system using finite-time input-to-state stability," *International Journal of Systems Science*, vol. 47, no. 10, pp. 2440–2448, 2016.

[11] X. Y. Zhou, "A chaotic system with invariable Lyapunov exponent and its circuit simulation," *Acta Physica Sinica*, vol. 60, no. 10, Article ID 100503, 2011.

[12] C. Li, K. Su, and J. Zhang, "Amplitude control and projective synchronization of a dynamical system with exponential nonlinearity," *Applied Mathematical Modelling: Simulation and Computation for Engineering and Environmental Systems*, vol. 39, no. 18, pp. 5392–5398, 2015.

[13] J. Jiang and Q. Qing Wu, "A New Three-Dimensional Chaotic System with Constant Exponent Spectrum: Analysis, Synchronization and Circuit Implementation," *Journal of Software* , vol. 11, no. 5, pp. 494–511, 2016.

[14] C. Li, L. Wu, H. Li, and Y. Tong, "A novel chaotic system and its topological horseshoe," *Nonlinear Analysis: Modelling and Control*, vol. 18, no. 1, pp. 66–77, 2013.

[15] L. Pan, W. Zhou, L. Zhou, and K. Sun, "Chaos synchronization between two different fractional-order hyperchaotic systems," *Communications in Nonlinear Science and Numerical Simulation*, vol. 16, no. 6, pp. 2628–2640, 2011.

[16] J. He, S. Yu, and J. Cai, "A method for image encryption based on fractional-order hyperchaotic systems," *Journal of Applied Analysis and Computation*, vol. 5, no. 2, pp. 197–209, 2015.

[17] M. P. Aghababa, "Fractional modeling and control of a complex nonlinear energy supply-demand system," *Complexity*, vol. 20, no. 6, pp. 74–86, 2015.

[18] Y. Wang, K. Sun, S. He, and H. Wang, "Dynamics of fractional-order sinusoidally forced simplified Lorenz system and its synchronization," *The European Physical Journal Special Topics*, vol. 223, no. 8, pp. 1591–1600, 2014.

[19] S. He, K. Sun, and H. Wang, "Complexity analysis and DSP implementation of the fractional-order Lorenz hyperchaotic system," *Entropy*, vol. 17, no. 12, pp. 8299–8311, 2015.

[20] J. Ruan, K. Sun, J. Mou, S. He, and L. Zhang, "Fractional-order simplest memristor-based chaotic circuit with new derivative," *The European Physical Journal Plus*, vol. 133, no. 1, 2018.

[21] V.-T. Pham, S. T. Kingni, C. Volos, S. Jafari, and T. Kapitaniak, "A simple three-dimensional fractional-order chaotic system without equilibrium: Dynamics, circuitry implementation, chaos control and synchronization," *AEÜ - International Journal of Electronics and Communications*, vol. 78, pp. 220–227, 2017.

[22] L. Zhang, K. Sun, W. Liu, and S. He, "A novel color image encryption scheme using fractional-order hyperchaotic system and DNA sequence operations," *Chinese Physics B*, vol. 26, no. 10, p. 100504, 2017.

[23] L. M. Pecora and T. L. Carroll, "Synchronization in chaotic systems," *Physical Review Letters*, vol. 64, no. 8, pp. 821–824, 1990.

[24] D. Xu and C. Y. Chee, "Controlling the ultimate state of projective synchronization in chaotic systems of arbitrary dimension," *Physical Review E: Statistical, Nonlinear, and Soft Matter Physics*, vol. 66, no. 4, 2002.

[25] M. G. Rosenblum, A. S. Pikovsky, and J. Kurths, "Phase synchronization of chaotic oscillators," *Physical Review Letters*, vol. 76, no. 11, pp. 1804–1807, 1996.

[26] A. Tayebi, S. Berber, and A. Swain, "Performance analysis of chaotic DSSS-CDMA synchronization under jamming attack," *Circuits, Systems and Signal Processing*, vol. 35, no. 12, pp. 4350–4371, 2016.

[27] A. Kajbaf, M. A. Akhaee, and M. Sheikhan, "Fast synchronization of non-identical chaotic modulation-based secure systems using a modified sliding mode controller," *Chaos, Solitons & Fractals*, vol. 84, pp. 49–57, 2016.

[28] I. Ahmad, A. Bin Saaban, A. B. Ibrahim, and M. Shahzad, "Global chaos synchronization of new chaotic system using linear active control," *Complexity*, vol. 21, no. 1, pp. 379–386, 2015.

[29] H. Saberi Nik, S. Effati, and J. Saberi-Nadjafi, "New ultimate bound sets and exponential finite-time synchronization for the complex Lorenz system," *Journal of Complexity*, vol. 31, no. 5, pp. 715–730, 2015.

[30] D. Ghosh and S. Bhattacharya, "Projective synchronization of new hyperchaotic system with fully unknown parameters," *Nonlinear Dynamics*, vol. 61, no. 1-2, pp. 11–21, 2010.

[31] S. Zheng, "Impulsive complex projective synchronization in drive-response complex coupled dynamical networks," *Nonlinear Dynamics*, vol. 79, no. 1, pp. 147–161, 2015.

[32] E. E. Mahmoud, "Modified projective phase synchronization of chaotic complex nonlinear systems," *Mathematics and Computers in Simulation*, vol. 89, pp. 69–85, 2013.

[33] W. Wang, I. Z. Kiss, and J. L. Hudson, "Experiments on arrays of globally coupled chaotic electrochemical oscillators: Synchronization and clustering," *Chaos: An Interdisciplinary Journal of Nonlinear Science*, vol. 10, no. 1, pp. 248–256, 2000.

[34] J. E. Rosa, W. B. Pardo, C. M. Ticos, J. A. Walkenstein, and M. Monti, "Phase synchronization of chaos in a plasma discharge tube," *International Journal of Bifurcation and Chaos*, vol. 10, no. 11, pp. 2551–2563, 2000.

[35] H. Wang, Q. Wang, Q. Lu, and Y. Zheng, "Equilibrium analysis and phase synchronization of two coupled HR neurons with gap junction," *Cognitive Neurodynamics*, vol. 7, no. 2, pp. 121–131, 2013.

[36] Z. Odibat, "A note on phase synchronization in coupled chaotic fractional order systems," *Nonlinear Analysis: Real World Applications*, vol. 13, no. 2, pp. 779–789, 2012.

[37] M. Caputo, "Linear models of dissipation whose Q is almost frequency independent-II," *Annals of Geophysics*, vol. 19, no. 4, pp. 529–539, 1966.

[38] K. Diethelm and N. J. Ford, "Analysis of fractional differential equations," *Journal of Mathematical Analysis and Applications*, vol. 265, no. 2, pp. 229–248, 2002.

[39] C. Li and H. Li, "Robust control for a class of chaotic and hyperchaotic systems via linear state feedback," *Physica Scripta*, vol. 85, no. 2, p. 025007, 2012.

[40] N. Aguila-Camacho, M. A. Duarte-Mermoud, and J. A. Gallegos, "Lyapunov functions for fractional order systems," *Communications in Nonlinear Science and Numerical Simulation*, vol. 19, no. 9, pp. 2951–2957, 2014.

[41] P. Zhou, H. Cai, and C. D. Yang, "Stabilization of the unstable equilibrium points of the fractional-order BLDCM chaotic system in the sense of Lyapunov by a single-state variable," *Nonlinear Dynamics*, vol. 84, no. 4, pp. 2357–2361, 2016.

[42] M. A. Duarte-Mermoud, N. Aguila-Camacho, J. A. Gallegos, and R. Castro-Linares, "Using general quadratic LYApunov functions to prove LYApunov uniform stability for fractional order systems," *Communications in Nonlinear Science and Numerical Simulation*, vol. 22, no. 1-3, pp. 650–659, 2015.

[43] Q. Wang, D. Ding, and D. Qi, "Mittag–Leffler synchronization of fractional-order uncertain chaotic systems," *Chinese Physics B*, vol. 24, no. 6, p. 060508, 2015.

[44] F. Li, W. Y. Jin, and J. Ma, "Modulation of nonlinear coupling on the synchronization induced by linear coupling," *Acta Physica Sinica*, vol. 61, no. 24, Article ID 240501, 2012.